Since January 2020 Elsevier has created a COVID-19 resource centre with free information in English and Mandarin on the novel coronavirus COVID-19. The COVID-19 resource centre is hosted on Elsevier Connect, the company's public news and information website.

Journal of Hazardous Materials 419 (2021) 126507

Contents lists available at ScienceDirect

Journal of Hazardous Materials

journal homepage: www.elsevier.com/locate/jhazmat

Research Paper

Uncovering the release of micro/nanoplastics from disposable face masks at times of COVID-19

Silvia Morgana [a,*], Barbara Casentini [b], Stefano Amalfitano [b]

[a] Institute for the Study of Anthropic Impact and Sustainability in the Marine Environment (IAS-CNR), Via della Vasca Navale, 00146 Rome, Italy
[b] Water Research Institute (IRSA-CNR), Via Salaria Km 29.300, Monterotondo, 00015 Rome, Italy

ARTICLE INFO

Editor: Dr. R Teresa

Keywords:
Microfibers
Nanoplastics
Water pollution
Microscopy
Flow cytometry

ABSTRACT

Wearing face masks is a fundamental prevention and control measure to limit the spread of COVID-19. The universal use and improper disposal of single-use face masks are raising serious concerns for their environmental impact, owing to the foregone contribution to plastic water pollution during and beyond the pandemic. This study aims to uncover the release of micro/nanoplastics generated from face mask nonwoven textiles once discarded in the aquatic environment. As assessed by microscopy and flow cytometry, the exposure to different levels of mechanical stress forces (from low to high shear stress intensities) was proved effective in breaking and fragmenting face mask fabrics into smaller debris, including macro-, micro-, and nano-plastics. Even at the low level of fabric deterioration following the first second of treatment, a single mask could release in water thousands of microplastic fibers and up to 10^8 submicrometric particles, mostly comprised in the nano-sized domain. By contributing to the current lack of knowledge regarding the potential environmental hazards posed by universal face masking, we provided novel quantitative data, through a suitable technological approach, on the release of micro/nanoplastics from single-use face masks that can threaten the aquatic ecosystems to which they finally end-up.

1. Introduction

The COVID-19 pandemic has been contrastingly but dramatically affecting human activities and natural environments at either global or local scale. Although lockdown measures are retained beneficial for the environment especially in areas at high anthropogenic pollution levels (Saadat et al., 2020; Zambrano-Monserrate et al., 2020), such environmental benefits are expected to be inherently provisional (Ragazzi et al., 2020). At the beginning of the pandemic, the World Health Organization estimated that the global demand for surgical masks, examination gloves, and protective screens stood respectively up to 89, 76, and 2 millions per month (World Health Organization, 2020). The use of masks, required against the primary aerial dispersal of SARS-CoV-2-containing droplets, has been made mandatory in most world regions, with such a high demand to rapidly overreach the local availability, distribution, and industrial production (Wu et al., 2020). In particular, the overproduction and universal use of disposable personal protective equipment have been challenging the plastic waste management, especially in developing countries (Chowdhury et al., 2021; Cordova et al., 2021; Torres and De-la-Torre, 2021).

Specifically intended for single use, face masks protect against aerial contaminants, including pollen, chemical fumes and pathogens. The filtering capacity and, hence, the level of protection depend on used materials and the engineering design. Despite differences among brands, face masks are generally made by assembling different layers of a thin nonwoven textile: a waterproof outer layer to repel fluids, a middle filtering layer to prevent particles and pathogen-containing droplets from penetrating in either direction, an inner layer of absorbent material to trap droplets from the user. The nonwoven fabric is obtained by bonding a mass of filaments together using heat, chemical, or mechanical means (spunbond and meltblown methods) to produce smooth, porous and highly durable sheets (Ding et al., 2020). Among the suitable plastic polymers, polypropylene is the most common used for assembling surgical mask, as it is relatively cheap and with low melt viscosity for easy processing (Chua et al., 2020).

Since the beginning of the COVID-19 pandemic, discarded face masks are reported to litter city streets, flow through sewage channels, float in sea water until reaching the bottom (Ardusso et al., 2021; De-la-Torre et al., 2021; Okuku et al., 2021), and risk evidences for local fauna were recently provided (Boyle, 2020; Gallo Neto et al., 2021).

* Corresponding author.
E-mail address: silvia.morgana@ias.cnr.it (S. Morgana).

https://doi.org/10.1016/j.jhazmat.2021.126507
Received 26 April 2021; Received in revised form 23 June 2021; Accepted 23 June 2021
Available online 26 June 2021

Under environmental conditions, plastic waste slowly degrade due to chemical, mechanical, and biological actions into micrometric and submicrometric plastic particles (Frias and Nash, 2019; Kwak and An, 2021). The smaller they are, the easier they can be ingested, accumulated and transferred by organisms along the food chain (B. Jiang et al., 2020). Ingestion of micrometric and submicrometric plastics is known to cause direct adverse effects (e.g., entanglement, suffocation) and to expose organisms to plastic-associated chemical and microbial agents with a prominent toxic and pathogenic potential (Sathicq et al., 2021; Vethaak and Leslie, 2016; Zhang and Xu, 2020).

Since the massive use of disposable face masks is likely to persist further beyond the current pandemic, there is urgent need to uncover all possible environmental repercussions. An increasing number of studies are pointing to face masks as an emerging source of plastic pollution that will shortly add-up to the already critical situation (Patrício Silva et al., 2021; Prata et al., 2021). First evidences of microplastic release from face masks are provided in the recent literature (Chen et al., 2021; Saliu et al., 2021), also detecting microfibers associated with chemical contaminants (Sullivan et al., 2021) and raising concern for their potential inhalation and ingestion risks (Li et al., 2021). However, there is still a lack of knowledge on the face mask contribution to micro/nanoplastic generation, given that microfibers can be fragmented into thousands of nano-sized particles, more persistent and difficult to be detected (Henry et al., 2019).

This study was intended to evaluate the potential release in water of micro/nanoplastics (MNPs) from the thin polypropylene (PP) textile used to assemble surgical face masks once discarded in the environment. More specifically, the aims were to (i) quantify the extent of plastic release from face mask fabrics at different levels of mechanical shear stress intensities, (ii) characterize morphologies and size of released micro/nanoplastics across a wide dimensional range (i.e., from millimeters downward nanometers) by microscopy and flow cytometry, (iii) provide evidence for potential implications of plastic pollution in water owing to the emerging issues posed by disposable plastic wastes at the time of COVID-19.

2. Material and methods

2.1. Experimental set-up: shear stress tests

The surgical face masks, purchased by GLF S.A.S. (Italy), consisted of 3 layers (i.e., inner, intermediate and outer) of PP spunbond nonwoven fabric with a density of 30 g/m^2. Sixteen masks were cut with scissors to remove the external welding and the elastic ear loops. The white intermediate nonwoven spunbond PP layer (hereafter named fabric) was manipulated with metal tweezers, sized and weighed on a high precision analytical balance (XS BL 303 E-balance, China). The sampled fabric was then placed in a glass beaker containing 500 mL of MilliQ water.

By adopting an experimental setup similar to that presented by Enfrin et al. (2020), a kitchen chopper (type HDP40; Kenwood, UK), equipped with a rotating blender blade (radius 11 cm) and operating at the maximum power (800 W), was used for a short-term shear damage process, specifically intended to mimic different levels of mechanical solicitation (i.e., from low to high shear stress intensities) that face masks can encounter once dispersed in the environment. The shear tests were carried out on different fabrics at increasing times and corresponding energy densities (1 s = 1.6 kJ/L, 15 s = 24 kJ/L, 30 s = 48 kJ/L, 60 s = 96 kJ/L, 120 s = 192 kJ/L), as estimated from known parameters (i.e., chopper power, treatment time, treated water volume) (Enfrin et al., 2020). Each test was repeated four times and included a preliminary control test performed with MilliQ water only (i.e., blank control). The beaker was carefully rinsed with MilliQ water (i.e., 5 times) in between each shear test to minimize external contamination.

Homogenous water aliquots were collected by a glass Pasteur pipette while keeping the beaker under manual agitation after each test. Sample aliquots were then analyzed by the methods described in the following sections.

The treated fabrics were collected from the beaker with tweezers, gently squeezed, and weighed after overnight drying at 40 °C. For each shear stress test, the fabric deterioration was measured in terms of weight loss percentage, as follows:

$$(W_1\text{-}W_2)/W_1 \times 100$$

where W_1 is the dry weight of the intact fabric (i.e., before blending), W_2 is the dry weight of the treated fabric (i.e., after blending).

2.2. Optic and epifluorescence microscopy for fabric texture characterization and microplastics analyses

The nonwoven fabric texture and filament web were inspected by a flat-field achromatic 40x magnification lens, mounted on a cell phone, with an optical resolution of approx. 2 μm (Tinyscope; https://www.tinyscope.com/ Wuhan, China). Upon calibration through a micrometric scale, a representative number of pictures (2.16 × 3.84 mm) were taken on intact and shear-damaged areas of dried fabrics to visually assess (i) density (i.e., number per unit area) and morphology (i.e., shape and size) of the breathability-related holes, (ii) thickness and integrity of PP filaments, with the help of digital magnification (up to 300 ×).

The occurrence of microplastics (MPs) released in water upon the shear tests (i.e., 16 samples) was assessed by an optical stereomicroscope (STEMI SR, Zeiss, Weet, Germany). Homogenous water aliquot (5 mL) was placed in a glass Petri dish and carefully inspected across a magnification range from 10 × to 50 ×. For each aliquot, the mostly recurrent particle types (i.e., homogeneous fibers excised from the filament web) were visually sorted, counted, and measured, until a minimum of 50 items were identified for each test (Morgana et al., 2018; Brandon et al., 2016). The visual identification allowed the detection of microfibers with a minimum size of 100 μm (hereafter named > 100 μm).

The LED fluorescence microscope CyScope HP (Sysmex Partec Italia s.r.l.), with an optical resolution of approx. 0.1 μm, employing transmitted light and fluorescence detection and equipped with UV and green excitation/emission sets, was used to qualitatively verify the occurrence of micrometric and submicrometric particles and check for their autofluorescence level. Briefly, sample aliquots (20 μL) were placed onto wells of a chambered slide (10-well epoxy-coated slides with well diameter of 6.7 mm – Thermo Scientific, Germany) and inspected at 400 × (in air) and 1000 × (mounting coverslip and using an immersion oil objective lens).

2.3. Flow cytometry for micro/nanoplastics counting and characterization

After the shear tests, sample aliquots (1 mL) from all samples (including blank controls) were collected into 2-mL Eppendorf tubes. Each aliquot was immediately treated with H_2O_2 30% (1:1 dilution), incubated at 40 °C and analyzed after 24 h from sampling. This pretreatment was applied to limit the occurrence of particulate organic matter that could interfere with plastic particle counting (Bessa et al., 2019).

All sample aliquots (including blank controls) were analyzed using a bench-top flow cytometer (A50-Micro; Apogee Flow Systems, Hertfordshire, UK), equipped with a solid-state UV laser (375 nm, 20 mV) and a blue laser (488 nm, 20 mV). According to the system specifications from the manufacturer, this flow cytometer is suitable to detect and quantify all suspended particles approximately from 0.08 μm to 100 μm, based on the light scatter signals and following a direct calibration with commercial solutions containing fluorescent beads at known size.

In this study, we used polystyrene yellow-green fluorescent calibration microspheres (Sub-micron Size Reference Kit, 10^6 green fluorescent beads/mL, Invitrogen™, F13839), with 5 different nominal diameters

(0.1 μm, 0.2 μm, 0.5 μm, 1.0 μm, 2.0 μm), as reference reagents to arrange voltages of photomultipliers (PMTs), threshold values, and the size-dependent gating strategy on histogram and density plots. The forward light scatter (FSC) was set at the lowest voltage (PMT = 200 V) to maximize the size range of detectable particles, while the side light scatter (SSC) was set at 350 V to obtain a better resolution for sizing submicrometric particles. PMTs on blue (430–470 nm), green (530/30 nm), orange (590/35), and red (> 610 nm) fluorescence channels were set at 410 V for the detection of fluorescent events. The analysis of micro/nanoplastics was performed exclusively under UV excitation for all samples (i.e., 44 runs including blank controls). Upon the analysis of MilliQ water, thresholding was set on the SSC channel and adjusted to move the background and instrumental noise below the first decade. Samples were run at low flow rates to keep the number of cytometric events below 1000 events/s and all acquired signals were plotted using the same settings.

Given the comparable refractive indexes of polystyrene and polypropylene (Shackelford, 2000) and according to the SSC peak signals (SSC-H ± 10%) of the calibration microspheres, we designed specific gates onto log-scaled cytograms for 4 size classes of plastic particles. By following the definition proposed by Gigault et al. (2018), we identified the classes "> 1.0″ (MPs with a nominal diameter ≥ 1.0 μm but smaller than then maximum analytical size of 100 μm), "0.5–1.0″ (NPs ≥ 0.5 μm but < 1 μm), "0.1–0.5″ (NPs ≥ 0.1 μm but < 0.5 μm), "< 0.1″ (NPs < 0.1 μm but larger than then minimum analytical size) (Fig. S1). A log-log density plot of signal peak versus area (i.e., FSC-H vs FSC-A) was used to visualize and assess the occurrence of non-spherical particles. The deviation from a linear relation between the two signal values allowed discriminating spherical (FSC-H = FSC-A) vs non-spherical particles (FSC-H < FSC-A).

Owing to the relevance of possible external contamination when detecting nanoparticles, MilliQ blank controls were included in each experimental run and treated same as samples. The specific background signals detected on the blank control (i.e., at each preliminary shear test performed with MilliQ water only) were subtracted from the concentration values of the target particles per each size class.

To assess the occurrence of microbial cells that could contribute to an overestimation of submicrometric particles by interfering across the targeted size range, the Total Cell Counts (TCC) were determined under blue laser excitation on the third untreated subset of sample replicates. Following a consolidated protocol described elsewhere (Amalfitano et al., 2018), aliquots (300 μL) were stained for 10 min in the dark at room temperature by SYBR Green I (1:10000 dilution; Life Technologies, code S7563). Thresholding was set at 10 fluorescence units on the green channel and microbial cells were quantified by their signature on the density plot of the side scatter vs the green fluorescence signals.

The volumetric absolute counting, expressed as events per mL (i.e., items/mL, cells/mL), and all supportive cytometric data (e.g., median values of FSC and SSC, percentage of non-spherical particles, percentage of autofluorescent particles) were extracted from designed gates by using the Apogee Histogram Software (v89.0). The.fcs files are freely available at the Flow Repository identifier: https://flowrepository.org/id/FR-FCM-Z462 https://flowrepository.org/xxx.

2.4. Data analysis and statistics

The concentration values of particles released in water after each shear test (items/mL) were referred to size (items/m^2) and weight (items/g) of the treated PP fabric. According to the manufacturer's specifics and product parameters, approximately 10 triple-layered face masks were obtained from one square meter of PP nonwoven textile. Therefore, all data of particle release were finally converted and shown as items/mask.

The correlation between the shear stress intensity, the percentage of fabric deterioration, and the release of particles was carried out using the Spearman's rho test. The statistical differences in micro/nanoplastic release at increasing shear stress intensities were assessed with the nonparametric Kruskal-Wallis test. The significance level for all analyses was set to 95% ($p = 0.05$). Statistical analysis was performed using IBM SPSS software (Version 20).

As previously invoked to explain the observed size distributions of plastics in aquatic environments (Brown and Wohletz, 1995; Timár et al., 2010), the sigmoid Weibull and lognormal distributions were applied to empirically model the plastic release, fragmentation, and agglomeration processes that may have occurred during the shear tests.

The relative contribution of the 5 size classes to the total retrieved particles was calculated and related to the shear test efficacy (i.e., particle concentration or weight vs applied energy density or percentage of weight loss after treatment). To estimate mass contribution to plastic budget, depending on the observed prevailing particles detected morphology, the mean volume (μm^3) was calculated by considering particles as spheres or as filaments, as follows:

$$\text{Microsphere mean volume } V = 4/3 \times \pi \times (D/2)^3$$

$$\text{Filament mean volume } V = (D/2)^2 \times \pi \times L$$

Where D is the nominal diameter and L the length of microscopy-detected particles. An approximate mean diameter was used for cytometry-detected particles within the size classes defined according to the calibration beads. The mean volume was then multiplied by the particle counts in each class and by the density of PP (900 kg/m^3) to estimate their contribution to the total mass.

2.5. Laboratory contamination control

Laboratory contamination was checked by adopting all precautions recommended to limit the overestimation of microplastic counts, including wearing of cotton clothing and laboratory coats. Glassware was thoroughly cleaned with MilliQ water. To check that no airborne contamination occurred in the laboratory, a blank control dish was left open on the lab bench and inspected at the optical stereomicroscope during the experiments (Wesch et al., 2017).

3. Results

3.1. Deterioration of PP fabric at increasing shear stress intensities

Before treatments, all the 16 nonwoven PP fabrics showed comparable size (approx. 135 × 130 × 0.125 mm), weight (549 ± 54 mg), and an intact texture with well-shaped rhomboid holes (approx. 0.6 mm^2), placed at a fixed distance (0.4 holes/mm^2) across a tangled web of PP filaments (20–30 μm in thickness). At increasing shear stress intensities, large areas of deterioration were found by visually inspecting the PP fabrics, with increasingly occurring shear-damaged holes and filaments resulting into a fuzzier fabric texture. This was particularly evident for samples subjected to higher shear stress levels (Fig. 1). A significant positive linear relation was found between the tissue deterioration level (% of weight loss) and the energy density (kJ/L) at increasing treatment times ($n = 16$; $r = 0.695$, $p = 0.003$) (Table 1), varying from 0.2 ± 0.3% (at the lowest shear intensity) to 3.2 ± 2.7% (at the highest). The water temperature raised from 17.5 °C to 21.0 °C at the end of the shear tests (120 s).

3.2. Counting and characterization of microplastics by optic stereomicroscopy

The release in water of fabric fragments and plastic particles, excised from the PP filament web, was observed (Fig. 2). The released MPs > 100 μm were fiber-like, with an average size of 1.7 ± 0.4 mm. Only few large fabric pieces were observed (> 5 mm, not considered in the counting). An increase in the formation of MPs (> 100 μm) was found across treatment time from 1 s (mean ± sd = 0.3 ± 0.1 × 10^5

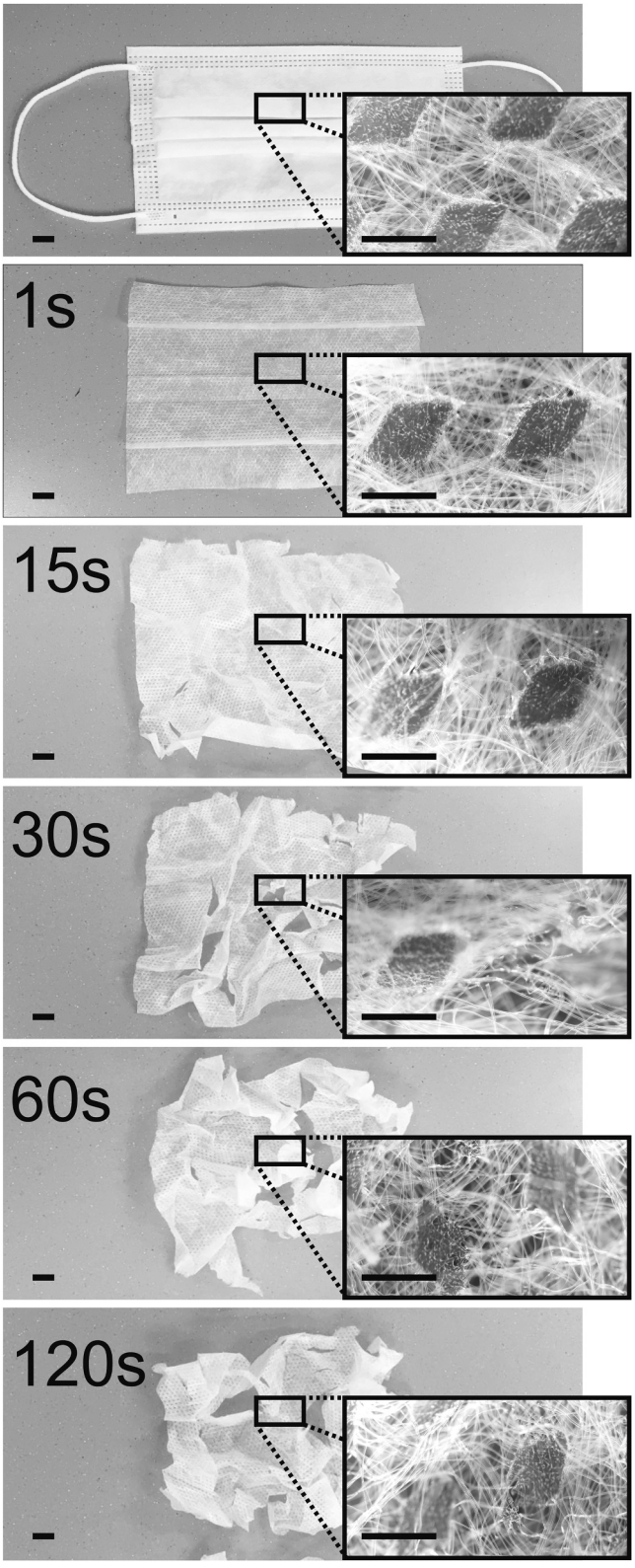

Fig. 1. Deterioration of PP fabric excised from a face mask at increasing treatment time (from 1 s to 120 s) and shear stress intensities (from 1.6 kJ/L to 192.0 kJ/L) (scale bar = 10 mm). 40 × Microscopic images (black boxes) show the intact and progressively damaged fabric texture (scale bar = 1 mm).

Table 1
Effects of shear stress intensity (i.e., treatment time and shear power) on fabric texture damage, water temperature (°C), and fabric deterioration (% of weight loss).

Shear time (s)	Energy density (kJ/L)	Water T (°C)	Weight loss (mg)	Fabric deterioration (%)
1	1.6	17.5	1.0 ± 1.6	0.2 ± 0.3
15	24.0	18.0	1.6 ± 1.0	0.3 ± 0.1
30	48.0	18.2	3.0 ± 0.2	0.6 ± 0.1
60[a]	96.0	19.1	11.2 ± 7.3	2.1 ± 1.4
120	192.0	21.0	15.6 ± 12.3	3.2 ± 2.7

Mean values (± standard deviation of triplicates) are reported.
[a] 4 replicates.

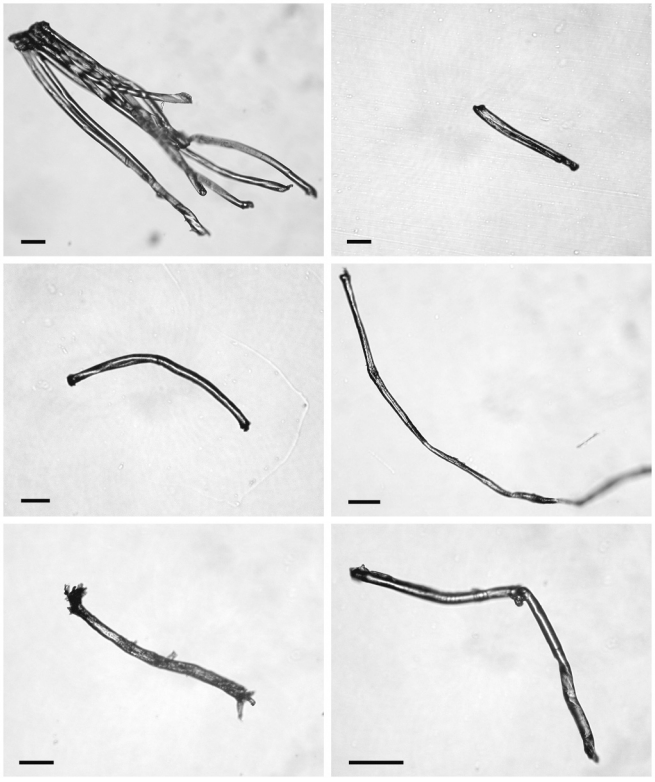

Fig. 2. Selected images of microplastic fragments and fibers excised from the PP filament web of the face mask fabric and released in water during the shear tests (scale bar = 0.1 mm).

items/m^2 of treated fabric, corresponding to 0.9 ± 0.2 × 10^3 items/g of PP) to 120 s (2.8 ± 0.5 × 10^5 items/m^2; 8.7 ± 1.5 × 10^3 items/g of PP). Overall, a single mask was found to release from 2.6 ± 0.7 × 10^3 items/mask (after 1 s) up to 2.8 ± 0.5 × 10^4 items/mask (after 120 s). The number of released MPs (> 100 μm) was significantly different according to the applied energy densities ($p = 0.010$) and followed a sigmoidal increase over treatment (Fig. 3).

3.3. Counting and characterization of micro/nanoplastics by flow cytometry

MNPs across a wide size range (0.1–100 μm) were visually spotted by microscopy and quantified by flow cytometry. A significant reduction of total counts was obtained by subtracting the unspecific signals detected in the blank controls at each shear test and size class (55.6 ± 19.6%). Moreover, following the SYBR Green staining protocol, the occurrence of microbial contamination was negligible and did not bias the particle counts (approx. 10^3 cells/mL). The mean value of total released particles

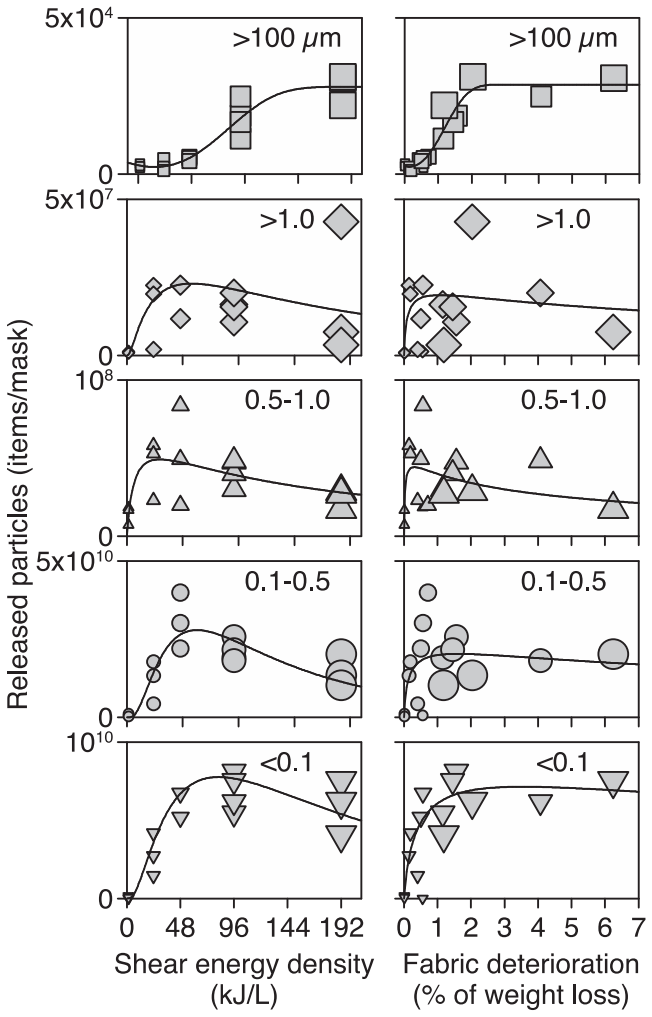

Fig. 3. Patterns of particle release from face mask fabric in water at increasing shear stress and fabric deterioration. Symbol size increases with treatment time. Sigmoid Weibull and lognormal distributions were applied to model the occurrence of particles within the 5 size classes.

was $2.1 \pm 1.4 \times 10^{11}$ items/m^2 of treated fabric, corresponding to $7.0 \pm 4.9 \times 10^{9}$ items/g of PP. The release of particles increased with energy density (kJ/L) and fabric deterioration across treatment times from 1 s ($7.6 \pm 4.6 \times 10^{9}$ items/m^2) to 30 s ($3.9 \pm 1.2 \times 10^{11}$ items/m^2), with a slight reduction afterward (60 s = $2.8 \pm 0.5 \times 10^{11}$ items/m^2; 120 s = $2.1 \pm 0.7 \times 10^{11}$ items/m^2). Overall, the average MNPs generated from single face mask ranged between $7.6 \pm 4.6 \times 10^{8}$ items/mask (after 1 s) up to $3.9 \pm 1.2 \times 10^{10}$ items/mask (after 30 s) (Fig. 3). MNPs release was found to be significantly different according to the applied energy density ($p = 0.017$). Despite higher shear intensities reflected greater fabric deterioration and particle release in water, the log-normal release of MNPs did not correlate with the sigmoidal increase of MPs > 100 μm over treatment.

By plotting the forward scatter peak and area signals (FSC-H vs FSC-A), the large majority of detected particles were spherical (FSC-H = FSC-A; > 99% of items within < 0.1 μm and 0.1–0.5 μm size classes) and non-fluorescent (blue channel < 10 fluorescence units). However, in 0.5–1.0 μm and > 1.0 μm size classes, the occurrence of non-spherical particles increased with treatment time (FSC-H < FSC-A; > 20% of total items at 120 s), along with the percentage of blue autofluorescent items (i.e., 65.5 ± 24.3% of total items in the > 1.0 μm size class).

Considering the relative distribution of released particles, the size classes 0.1–0.5 μm and < 0.1 μm were the most represented in numerical terms (78.9 ± 6.5% and 20.5 ± 7.5% of total items, respectively). Conversely, in terms of mass weight, the size classes > 100 μm and > 1.0 μm contributed the most to the total retrieved mass (64.3 ± 24.7% and 26.1 ± 18.4% of total mass, respectively) (Fig. 4).

4. Discussion

This study was entailed to assess the release in water of micro/nanoplastics generated from single-use face masks once discarded in the environment and exposed to mechanical stress forces. A two-blade impeller was used to induce the deterioration of face mask nonwoven textile at increasing shear stress intensities, from low (1.6 kJ/L) to high (192 kJ/L) levels, through short-term experimental tests. The applied forces were significantly lower than those used in a similar experimental set-up for breaking down large plastics (11 MJ/L) (Ekvall et al., 2019), and in line with values reported for wastewater treatment plants (10–150 kJ/L) (Enfrin et al., 2020). In WWTPs and engineered water systems, strong mechanical solicitations can be applied to plastic debris flowing along with influent samples at different stages of the treatment process (e.g., grid and grit chambers, aeration and sedimentation tanks), which are reported as a consistent source of microplastic release (Enfrin et al., 2019; Jiang et al., 2020). In environment, the mechanical deterioration of PP textile can be promoted by collision with rocks and sands caused by mechanical forces (e.g., wind, waves, tides). The energy density of such environmental events was estimated between 0.5 and 50 J/m^3 of air/water (Layton, 2008), thus falling within the range of those (Enfrin et al., 2019) used in this study. On land, frictional stresses generated by abrasion with the road surface can easily overcome the limiting strength of the nonwoven textile, resulting in micro-cutting of the face mask fabric (Zhang et al., 2021). Precipitation, weathering, surface runoff, water flow acting on river bed, bottom currents upon the sea floor, waves-rocks interaction, but also the transport through pipes, drains, and water treatment steps, are reported as the main routes driving plastic transfer and mechanical deterioration (Duan et al., 2021; Kane et al., 2020; Zhang et al., 2021). Face mask deterioration will largely depend on local hydrodynamic conditions, with an estimated time of tens to hundreds years for the full decomposition of plastic components (Chamas et al., 2020). In this study, the increasing stress forces were responsible for an average fabric deterioration of

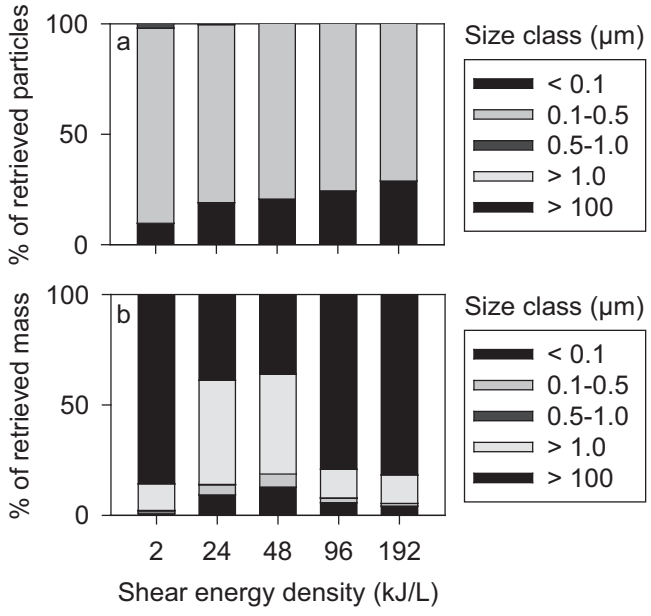

Fig. 4. Relative contribution to total number (a) and weight mass (b) of detected micro/nanoplastics released in water during the shear tests. Conversion in weight was based on particle morphology and mean size within the 5 size classes.

1.2 ± 1.3% of the initial weight, corresponding to a mean weight loss of 6.8 ± 8.2 mg. Despite an overall low weight loss (i.e., 1.0 ± 1.6 mg at the lowest force applied), a consistent number of micro/nanoplastics was immediately released in water following the first second of treatment, and subsequently with different trends according to particle size and shape. Considering that weight change alone was likely not suitable for characterizing the plastic deterioration process, we underline the importance of understanding and assessing the micro/nanoplastic release.

At the lowest mechanical stress (i.e., 1.6 kJ/L, comparable to wind energy on a moderately windy day or slow tidal movement, Layton (2008), a single triple layered-face mask is estimated to generate $2.6 \pm 0.7 \times 10^3$ microfibers (> 100 μm) with an average length of 1.7 ± 0.4 mm. In line with our findings despite the different experimental configurations, recent studies reported thousands of microfibers/mask released in water, mostly ranging between 0.1 mm and 1 mm (Chen et al., 2021; Saliu et al., 2021).

According to flow cytometry data, the average amount of micro/nanoplastics (0.1–100 μm) generated from disposable face masks across the treatments ($2.1 \pm 1.4 \times 10^{10}$ items/mask) were almost six order of magnitude higher than the average released MPs (> 100 μm). Apparently following a fragmentation process, we found a general prevalence of spherical nanoparticles in the size class 0.1–0.5 μm, followed by the smallest size class (< 0.1 μm) at higher energy densities. Although further confirmations are needed, the fragmentation rate of face mask fabrics can be higher than that determined in this study, since several complex factors may co-occur in the environment and accelerate the overall plastic deterioration (Julienne et al., 2019). Moreover, the total release of micro/nanoplastics was not linearly correlated with weight loss and deterioration of the treated fabrics, but rather followed a lognormal curve at increasing shear stress. These findings could point either to technical detection issues, since large fabric fragments (i.e., > 5 mm) and small nanoparticles (i.e., < 80 nm) were not reliably quantified, or to the density-dependent aggregation/agglomeration of the newly-formed nanoplastics, as also reported in experimental and field studies (Singh et al., 2019). Both fragmentation and agglomeration processes could be evoked to explain the different release trends observed between the target particle size classes.

Notably, blue autofluorescence signals were detected for micrometric particles (> 1.0 μm) and decreased with size. Some plastic particles were reported to show detectable levels of autofluorescence, after excitement by near UV or visible radiation (e.g., polycarbonate, poly (methyl-methacrylate), poly(dimethylsiloxane), cyclo-olefin copolymer) (Kaile et al., 2020; Piruska et al., 2005), which can be amplified upon specific thermal/chemical treatments (Monteleone et al., 2021; Young et al., 2013). Overall, such phenomenon has inherent implications in particle detection, and the autofluorescence properties, coupled with secondary staining techniques, deserve to be further explored to improve the identification and characterization of a large fraction of the micro/nanoplastic pool (Kaile et al., 2020).

Given the rapid advancement of plastic detection methods and the relative simplicity in designing deterioration tests under controlled laboratory conditions (Lambert and Wagner, 2016; Mattsson et al., 2021; Song et al., 2017), the experimental approach is likely to represent a fundamental first step to provide reproducible evidences on the fate and potential implications of plastic materials ending-up into aquatic systems.

Among the numerous gaps affecting the current knowledge on micro/nanoplastic research, including environmental presence, transport pathways, adsorption of contaminants, and even the definition of size limits (Frias and Nash, 2019), there is not a general consensus on detection methods (Caputo et al., 2021). We showed the potential application of flow cytometry for detecting micrometric and submicrometric plastic particles. Yet rarely considered for non-biological targets, this technology has been successfully applied to detect small plastic particles in aquatic media (Bringer et al., 2020; Kaile et al., 2020; Le Bihanic et al., 2020), with performances comparable to those showed by other more established analytical techniques (e.g., dynamic light scattering, nanoparticle tracking analysis) (Caputo et al., 2021). FCM was suitable for detecting homogenously distributed particles in liquid suspensions, albeit challenging when applied to environmental and biological complex matrices. Staining with selective dyes (e.g., Nile Red), after appropriate treatments for organic matter digestion, has been proposed as promising methodology coupled with flow cytometry to identify plastic particles from heterogeneous matrices (Kaile et al., 2020). However, chemical characterization still remains a relevant limitation to be addressed when working with environmental samples to distinguish among different plastic polymer types. In the present work, a particular attention has been directed toward removing all potential sources of particle quantification bias. The subtraction of false positive signals detected with FCM in blank control samples (55.6 ± 19.6% of total counted items) confirmed the fundamental need for quality controls, especially when working within the nano-size range. Taking advantage from the available literature on MNPs (Enfrin et al., 2020; Kaile et al., 2020; Prata et al., 2021), we carefully included a series of steps (i.e., a thoroughly washing of all FCM fluidics between each treatment, sample digestion in H_2O_2) to avoid particle count overestimation. Hence, for the purpose of this experimental study, FCM was proved to be a flexible, nearly real-time (i.e., time to results < 20 min from sampling) and reliable (i.e., thousands of events counted per second) technology to quantify plastic particles released from face masks across a wide dimensional range.

Global estimates reported that more than 10 million masks can reach the oceans monthly, with a total weight of 30–40 tons (Adyel, 2020). Basing on our findings and considering that discarded face masks can promptly deteriorate through varying environmental stressors and different mechanical forces, this translates into 10^{11} microfibers and 10^{18} micro/nanoplastics potentially entering the aquatic ecosystem per day. Such extrapolation of experimental data must be used with due caution, but it clearly suggests that universal face masking will likely add further burden to the current plastic pollution level in water. As nonwoven textiles used for disposable protective equipment and sanitary products (e.g., wet wipes and sanitary towels) are emerging as potential new sources of micro/nanoplastics (Ó Briain et al., 2020; Shruti et al., 2020), it is deemed critical to include face masks in plastic pollution research for a more accurate projection of the global plastic budget.

5. Conclusions

By mimicking conditions of weathering under realistic intensity levels of mechanical deterioration, our experimental results revealed that a consistent high number of micro/nanoplastics can be promptly released from a single mask, despite an overall low level of fabric deterioration (average 1.2 ± 1.3% of the initial weight). Flow cytometry was successfully applied to quantify the release of spherical submicrometric particles from discarded face mask fabrics, at values ($2.1 \pm 1.4 \times 10^{10}$ items/mask) notably higher than those found for microplastics (> 100 μm) by microscopy ($1.2 \pm 1.07 \times 10^4$ items/mask). Moreover, we found a predominant release of small plastic particles, mostly comprised in the nano-sized (size classes 0.1–0.5 μm and < 0.1 μm), which belong to the fraction of plastic fragments more easily ingested by aquatic organisms with direct access and magnification through the aquatic food web.

CRediT authorship contribution statement

Silvia Morgana: Investigation, Writing - review & editing. **Barbara Casentini**: Conceptualization, Writing - review & editing. **Stefano Amalfitano**: Conceptualization, Investigation, Writing - review & editing.

Declaration of Competing Interest

The authors declare that they have no known competing financial interests or personal relationships that could have appeared to influence the work reported in this paper.

Acknowledgements

The Authors thank Massimo Sanchez and Valentina Tirelli of the Flow Cytometry Area (Core Facilities, Italian Institute of Health - ISS) for providing technical support and valuable advice on the interpretation of flow cytometric data. The experimental activities were partly supported by the projects GO-FOR-WATER (ERA-NET FLAG ERA III, n. 825207) and GRAPHIL (GrapheneCore3-H2020-SGA-FET-GRAPHENE, n. 881603).

Appendix A. Supporting information

Supplementary data associated with this article can be found in the online version at doi:10.1016/j.jhazmat.2021.126507.

References

Adyel, T.M., 2020. Accumulation of plastic waste during COVID-19. Science 369, 1314–1315. https://doi.org/10.1126/science.abd9925.

Amalfitano, S., Fazi, S., Ejarque, E., Freixa, A., Romaní, A.M., Butturini, A., 2018. Deconvolution model to resolve cytometric microbial community patterns in flowing waters. Cytom. Part A 93, 194–200. https://doi.org/10.1002/cyto.a.23304.

Ardusso, M., Forero-López, A.D., Buzzi, N.S., Spetter, C.V., Fernández-Severini, M.D., 2021. COVID-19 pandemic repercussions on plastic and antiviral polymeric textile causing pollution on beaches and coasts of South America. Sci. Total Environ. 763, 144365 https://doi.org/10.1016/j.scitotenv.2020.144365.

Bessa, F., Kogel, T., Frias, J., Lusher, A., 2019. Harmonized protocol for monitoring microplastics in biota, Micropoll-Multilevel assessment of microplastics and associated pollutants in the Baltic Sea View project. doi:10.13140/RG.2.2.28588.72321/1.

Boyle, L., 2020. Bird dies after getting tangled in coronavirus face mask, The Independent, The Independent [WWW Document]. Independent.

Brandon, J., Goldstein, M., Ohman, M.D., 2016. Long-term aging and degradation of microplastic particles: comparing in situ oceanic and experimental weathering patterns. Mar. Pollut. Bull. 110, 299–308. https://doi.org/10.1016/j.marpolbul.2016.06.048.

Bringer, A., Thomas, H., Prunier, G., Dubillot, E., Bossut, N., Churlaud, C., Clérandeau, C., Le Bihanic, F., Cachot, J., 2020. High density polyethylene (HDPE) microplastics impair development and swimming activity of Pacific oyster D-larvae, Crassostrea gigas, depending on particle size. Environ. Pollut. 260, 113978 https://doi.org/10.1016/j.envpol.2020.113978.

Brown, W.K., Wohletz, K.H., 1995. Derivation of the Weibull distribution based on physical principles and its connection to the Rosin–Rammler and lognormal distributions. J. Appl. Phys. 78, 2758–2763. https://doi.org/10.1063/1.360073.

Caputo, F., Vogel, R., Savage, J., Vella, G., Law, A., Della Camera, G., Hannon, G., Peacock, B., Mehn, D., Ponti, J., Geiss, O., Aubert, D., Prina-Mello, A., Calzolai, L., 2021. Measuring particle size distribution and mass concentration of nanoplastics and microplastics: addressing some analytical challenges in the sub-micron size range. J. Colloid Interface Sci. 588, 401–417. https://doi.org/10.1016/j.jcis.2020.12.039.

Chamas, A., Moon, H., Zheng, J., Qiu, Y., Tabassum, T., Jang, J.H., Abu-Omar, M., Scott, S.L., Suh, S., 2020. Degradation rates of plastics in the environment. ACS Sustain. Chem. Eng. 8, 3494–3511. https://doi.org/10.1021/acssuschemeng.9b06635.

Chen, Xianchuan, Chen, Xiaofei, Liu, Q., Zhao, Q., Xiong, X., Wu, C., 2021. Used disposable face masks are significant sources of microplastics to environment. Environ. Pollut. 285, 117485 https://doi.org/10.1016/j.envpol.2021.117485.

Chowdhury, H., Chowdhury, T., Sait, S.M., 2021. Estimating marine plastic pollution from COVID-19 face masks in coastal regions. Mar. Pollut. Bull. 168, 112419 https://doi.org/10.1016/j.marpolbul.2021.112419.

Chua, M.H., Cheng, W., Goh, S.S., Kong, J., Li, B., Lim, J.Y.C., Mao, L., Wang, S., Xue, K., Yang, L., Ye, E., Zhang, K., Cheong, W.C.D., Tan, Beng Hoon, Li, Z., Tan, Ban Hock, Loh, X.J., 2020. Face masks in the new COVID-19 normal: materials, testing, and perspectives. Research 2020, 1–40. https://doi.org/10.34133/2020/7286735.

Cordova, M.R., Nurhati, I.S., Riani, E., Nurhasanah, Iswari, M.Y., 2021. Unprecedented plastic-made personal protective equipment (PPE) debris in river outlets into Jakarta Bay during COVID-19 pandemic. Chemosphere 268, 129360. https://doi.org/10.1016/j.chemosphere.2020.129360.

De-la-Torre, G.E., Rakib, M.R.J., Pizarro-Ortega, C.I., Dioses-Salinas, D.C., 2021. Occurrence of personal protective equipment (PPE) associated with the COVID-19 pandemic along the coast of Lima, Peru. Sci. Total Environ. 774, 145774 https://doi.org/10.1016/j.scitotenv.2021.145774.

Ding, Z., Babar, A.A., Wang, C., Zhang, P., Wang, X., Yu, J., Ding, B., 2021. Spunbonded needle-punched nonwoven geotextiles for filtration and drainage applications: manufacturing and structural design. Compos. Commun. 25, 100481 https://doi.org/10.1016/j.coco.2020.100481.

Duan, J., Bolan, N., Li, Y., Ding, S., Atugoda, T., Vithanage, M., Sarkar, B., Tsang, D.C.W., Kirkham, M.B., 2021. Weathering of microplastics and interaction with other coexisting constituents in terrestrial and aquatic environments. Water Res 196, 117011. https://doi.org/10.1016/j.watres.2021.117011.

Ekvall, M.T., Lundqvist, M., Kelpsiene, E., Šileikis, E., Gunnarsson, S.B., Cedervall, T., 2019. Nanoplastics formed during the mechanical breakdown of daily-use polystyrene products. Nanoscale Adv. 1, 1055–1061. https://doi.org/10.1039/C8NA00210J.

Enfrin, M., Dumée, L.F., Lee, J., 2019. Nano/microplastics in water and wastewater treatment processes – origin, impact and potential solutions. Water Res. 161, 621–638. https://doi.org/10.1016/j.watres.2019.06.049.

Enfrin, M., Lee, J., Gibert, Y., Basheer, F., Kong, L., Dumée, L.F., 2020. Release of hazardous nanoplastic contaminants due to microplastics fragmentation under shear stress forces. J. Hazard. Mater. 384, 121393 https://doi.org/10.1016/j.jhazmat.2019.121393.

Frias, J.P.G.L., Nash, R., 2019. Microplastics: finding a consensus on the definition. Mar. Pollut. Bull. 138, 145–147. https://doi.org/10.1016/j.marpolbul.2018.11.022.

Gallo Neto, H., Gomes Bantel, C., Browning, J., Della Fina, N., Albuquerque Ballabio, T., Teles de Santana, F., de Karam e Britto, M., Beatriz Barbosa, C., 2021. Mortality of a juvenile Magellanic penguin (Spheniscus magellanicus, Spheniscidae) associated with the ingestion of a PFF-2 protective mask during the Covid-19 pandemic. Mar. Pollut. Bull. 166, 112232 https://doi.org/10.1016/j.marpolbul.2021.112232.

Gigault, J., Halle, A., ter, Baudrimont, M., Pascal, P.-Y., Gauffre, F., Phi, T.-L., El Hadri, H., Grassl, B., Reynaud, S., 2018. Current opinion: what is a nanoplastic? Environ. Pollut. 235, 1030–1034. https://doi.org/10.1016/j.envpol.2018.01.024.

Henry, B., Laitala, K., Klepp, I.G., 2019. Microfibres from apparel and home textiles: prospects for including microplastics in environmental sustainability assessment. Sci. Total Environ. 652, 483–494. https://doi.org/10.1016/j.scitotenv.2018.10.166.

Jiang, B., Kauffman, A.E., Li, L., McFee, W., Cai, B., Weinstein, J., Lead, J.R., Chatterjee, S., Scott, G.I., Xiao, S., 2020. Health impacts of environmental contamination of micro- and nanoplastics: a review. Environ. Health Prev. Med. 25, 29. https://doi.org/10.1186/s12199-020-00870-9.

Jiang, J., Wang, X., Ren, H., Cao, G., Xie, G., Xing, D., Liu, B., 2020. Investigation and fate of microplastics in wastewater and sludge filter cake from a wastewater treatment plant in China. Sci. Total Environ. 746, 141378 https://doi.org/10.1016/j.scitotenv.2020.141378.

Julienne, F., Delorme, N., Lagarde, F., 2019. From macroplastics to microplastics: role of water in the fragmentation of polyethylene. Chemosphere 236, 124409. https://doi.org/10.1016/j.chemosphere.2019.124409.

Kaile, N., Lindivat, M., Elio, J., Thuestad, G., Crowley, Q.G., Hoell, I.A., 2020. Preliminary results from detection of microplastics in liquid samples using flow cytometry. Front. Mar. Sci. 7, 7. https://doi.org/10.3389/fmars.2020.552688.

Kane, I.A., Clare, M.A., Miramontes, E., Wogelius, R., Rothwell, J.J., Garreau, P., Pohl, F., 2020. Seafloor microplastic hotspots controlled by deep-sea circulation. Science 368, 1140–1145. https://doi.org/10.1126/science.aba5899.

Kwak, J. Il, An, Y.-J., 2021. Post COVID-19 pandemic: biofragmentation and soil ecotoxicological effects of microplastics derived from face masks. J. Hazard. Mater. 416, 126169 https://doi.org/10.1016/j.jhazmat.2021.126169.

Lambert, S., Wagner, M., 2016. Characterisation of nanoplastics during the degradation of polystyrene. Chemosphere 145, 265–268. https://doi.org/10.1016/j.chemosphere.2015.11.078.

Layton, B.E., 2008. A comparison of energy densities of prevalent energy sources in units of joules per cubic meter. Int. J. Green Energy 5, 438–455. https://doi.org/10.1080/15435070802498036.

Le Bihanic, F., Clérandeau, C., Cormier, B., Crebassa, J.-C., Keiter, S.H., Beiras, R., Morin, B., Bégout, M.-L., Cousin, X., Cachot, J., 2020. Organic contaminants sorbed to microplastics affect marine medaka fish early life stages development. Mar. Pollut. Bull. 154, 111059 https://doi.org/10.1016/j.marpolbul.2020.111059.

Li, L., Zhao, X., Li, Z., Song, K., 2021. COVID-19: performance study of microplastic inhalation risk posed by wearing masks. J. Hazard. Mater. 411, 124955 https://doi.org/10.1016/j.jhazmat.2020.124955.

Mattsson, K., Björkroth, F., Karlsson, T., Hassellöv, M., 2021. Nanofragmentation of expanded polystyrene under simulated environmental weathering (thermooxidative degradation and hydrodynamic turbulence). Front. Mar. Sci. 7 https://doi.org/10.3389/fmars.2020.578178.

Monteleone, A., Brandau, L., Schary, W., Wenzel, F., 2021. Using autofluorescence for microplastic detection – heat treatment increases the autofluorescence of microplastics1. Clin. Hemorheol. Microcirc. 76, 473–493. https://doi.org/10.3233/CH-209223.

Morgana, S., Ghigliotti, L., Estévez-Calvar, N., Stifanese, R., Wieckzorek, A., Doyle, T., Christiansen, J.S., Faimali, M., Garaventa, F., 2018. Microplastics in the Arctic: a case study with sub-surface water and fish samples off Northeast Greenland. Environ. Pollut. 242, 1078–1086. https://doi.org/10.1016/j.envpol.2018.08.001.

Ó Briain, O., Marques Mendes, A.R., McCarron, S., Healy, M.G., Morrison, L., 2020. The role of wet wipes and sanitary towels as a source of white microplastic fibres in the marine environment. Water Res. 182, 116021 https://doi.org/10.1016/j.watres.2020.116021.

Okuku, E., Kiteresi, L., Owato, G., Otieno, K., Mwalugha, C., Mbuche, M., Gwada, B., Nelson, A., Chepkemboi, P., Achieng, Q., Wanjeri, V., Ndwiga, J., Mulupi, L., Omire, J., 2021. The impacts of COVID-19 pandemic on marine litter pollution along the Kenyan Coast: a synthesis after 100 days following the first reported case in

Kenya. Mar. Pollut. Bull. 162, 111840 https://doi.org/10.1016/j.marpolbul.2020.111840.
Patrício Silva, A.L., Prata, J.C., Walker, T.R., Duarte, A.C., Ouyang, W., Barcelò, D., Rocha-Santos, T., 2021. Increased plastic pollution due to COVID-19 pandemic: challenges and recommendations. Chem. Eng. J. 405, 126683 https://doi.org/10.1016/j.cej.2020.126683.
Piruska, A., Nikcevic, I., Lee, S.H., Ahn, C., Heineman, W.R., Limbach, P.A., Seliskar, C.J., 2005. The autofluorescence of plastic materials and chips measured under laser irradiation. Lab Chip 5, 1348–1354. https://doi.org/10.1039/b508288a.
Prata, J.C., Reis, V., da Costa, J.P., Mouneyrac, C., Duarte, A.C., Rocha-Santos, T., 2021. Contamination issues as a challenge in quality control and quality assurance in microplastics analytics. J. Hazard. Mater. 403, 123660 https://doi.org/10.1016/j.jhazmat.2020.123660.
Ragazzi, M., Rada, E.C., Schiavon, M., 2020. Municipal solid waste management during the SARS-COV-2 outbreak and lockdown ease: lessons from Italy. Sci. Total Environ. 745, 141159 https://doi.org/10.1016/j.scitotenv.2020.141159.
Saadat, S., Rawtani, D., Hussain, C.M., 2020. Environmental perspective of COVID-19. Sci. Total Environ. 728, 138870 https://doi.org/10.1016/j.scitotenv.2020.138870.
Saliu, F., Veronelli, M., Raguso, C., Barana, D., Galli, P., Lasagni, M., 2021. The release process of microfibers: from surgical face masks into the marine environment. Environ. Adv. 4, 100042 https://doi.org/10.1016/j.envadv.2021.100042.
Sathicq, M.B., Sabatino, R., Corno, G., Di Cesare, A., 2021. Are microplastic particles a hotspot for the spread and the persistence of antibiotic resistance in aquatic systems? Environ. Pollut. 279, 116896 https://doi.org/10.1016/j.envpol.2021.116896.
Shackelford, J.F., 2000. Materials Science for Engineers. Upper Saddle River, New Jersey.
Shruti, V.C., Pérez-Guevara, F., Elizalde-Martínez, I., Kutralam-Muniasamy, G., 2020. Reusable masks for COVID-19: a missing piece of the microplastic problem during the global health crisis. Mar. Pollut. Bull. 161, 111777 https://doi.org/10.1016/j.marpolbul.2020.111777.
Singh, N., Tiwari, E., Khandelwal, N., Darbha, G.K., 2019. Understanding the stability of nanoplastics in aqueous environments: effect of ionic strength, temperature, dissolved organic matter, clay, and heavy metals. Environ. Sci. Nano 6, 2968–2976. https://doi.org/10.1039/C9EN00557A.
Song, Y.K., Hong, S.H., Jang, M., Han, G.M., Jung, S.W., Shim, W.J., 2017. Combined effects of UV exposure duration and mechanical abrasion on microplastic fragmentation by polymer type. Environ. Sci. Technol. 51, 4368–4376. https://doi.org/10.1021/acs.est.6b06155.
Sullivan, G.L., Delgado-Gallardo, J., Watson, T.M., Sarp, S., 2021. An investigation into the leaching of micro and nano particles and chemical pollutants from disposable face masks - linked to the COVID-19 pandemic. Water Res. 196, 117033 https://doi.org/10.1016/j.watres.2021.117033.
Timár, G., Blömer, J., Kun, F., Herrmann, H.J., 2010. New Universality class for the fragmentation of plastic materials. Phys. Rev. Lett. 104, 095502 https://doi.org/10.1103/PhysRevLett.104.095502.
Torres, F.G., De-la-Torre, G.E., 2021. Face mask waste generation and management during the COVID-19 pandemic: an overview and the Peruvian case. Sci. Total Environ. 786, 147628 https://doi.org/10.1016/j.scitotenv.2021.147628.
Vethaak, A.D., Leslie, H.A., 2016. Plastic debris is a human health issue. Environ. Sci. Technol. 50, 6825–6826. https://doi.org/10.1021/acs.est.6b02569.
Wesch, C., Elert, A.M., Wörner, M., Braun, U., Klein, R., Paulus, M., 2017. Assuring quality in microplastic monitoring: about the value of clean-air devices as essentials for verified data. Sci. Rep. 7, 5424. https://doi.org/10.1038/s41598-017-05838-4.
World Health Organization, 2020. Shortage of personal protective equipment endangering health workers worldwide, World Heal. Organ.
Wu, H., Huang, J., Zhang, C.J.P., He, Z., Ming, W.-K., 2020. Facemask shortage and the novel coronavirus disease (COVID-19) outbreak: Reflections on public health measures. EClinicalMedicine 21, 100329. https://doi.org/10.1016/j.eclinm.2020.100329.
Young, E.W.K., Berthier, E., Beebe, D.J., 2013. Assessment of enhanced autofluorescence and impact on cell microscopy for microfabricated thermoplastic devices. Anal. Chem. 85, 44–49. https://doi.org/10.1021/ac3034773.
Zambrano-Monserrate, M.A., Ruano, M.A., Sanchez-Alcalde, L., 2020. Indirect effects of COVID-19 on the environment. Sci. Total Environ. 728, 138813 https://doi.org/10.1016/j.scitotenv.2020.138813.
Zhang, K., Hamidian, A.H., Tubić, A., Zhang, Y., Fang, J.K.H., Wu, C., Lam, P.K.S., 2021. Understanding plastic degradation and microplastic formation in the environment: a review. Environ. Pollut. 274, 116554 https://doi.org/10.1016/j.envpol.2021.116554.
Zhang, M., Xu, L., 2020. Transport of micro- and nanoplastics in the environment: Trojan-Horse effect for organic contaminants. Crit. Rev. Environ. Sci. Technol. 1–37. https://doi.org/10.1080/10643389.2020.1845531.